Selective Oxidation of Furfural to Succinic Acid Over Lewis Acidic Sn-Beta

Yayati Naresh Palai,[†,‡] Abhijit Shrotri,[,†] Atsushi Fukuoka[*,†]*

[†]Institute for Catalysis, Hokkaido University, Kita 21 Nishi 10, Kita-ku, Sapporo, Hokkaido 001-0021, Japan, ashrotri@cat.hokudai.ac.jp, fukuoka@cat.hokudai.ac.jp

[‡]Graduate School of Chemical Sciences and Engineering, Hokkaido University, Kita 13 Nishi 8, Kita-ku, Sapporo, Hokkaido 060-8628, Japan

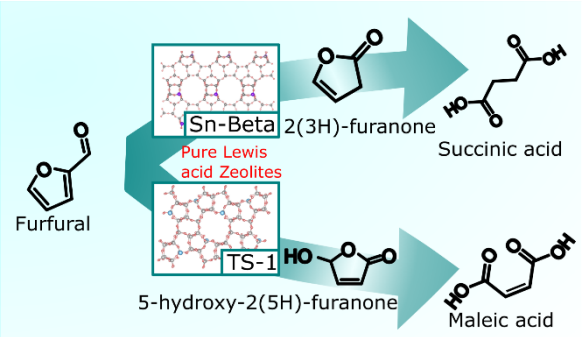

ABSTRACT

Selective production of succinic acid from furfural with H_2O_2 over Sn-Beta, a pure Lewis acid catalyst, is reported. Under optimized reaction conditions 53 % yield of succinic acid was obtained and the catalyst was recyclable. 2(3H)-Furanone was detected as an intermediate using ^{1}H NMR, HH COSY NMR, LC-MS and GC-MS. Kinetic modeling revealed that Baeyer-Villiger oxidation of furfural to 2(3H)-furanone was accelerated in comparison to other competing reactions in the presence of purely Lewis acidic Sn-Beta catalyst. The Lewis acid density of Sn-Beta catalyst was directly correlated to formation rate of products,

confirming a Lewis acid catalyzed mechanism. Detailed characterization showed that Sn-Beta activates furfural by coordinating to the carbonyl group and does not activate H_2O_2. On the other hand, parent HBeta-38 zeolite produced activated H_2O_2 in solution, which caused side reactions to produce maleic acid. Selectivity of Sn-Beta was also compared with TS-1, another Lewis acid zeolite, which produced maleic acid because of the ability of TS-1 to activate H_2O_2 as hydroperoxy species. Therefore, Sn-Beta is a selective and reusable catalyst for succinic acid synthesis from biomass derived furfural.

Keywords: Furfural oxidation, Sn-Beta zeolite, Succinic acid, Baeyer-villiger oxidation, Lewis acid

Introduction

Succinic acid is a four-carbon dicarboxylic acid with versatile industrial application. The global market for succinic acid is expected to grow from US$132 to US$183 million during a period of 2018 to 2023 at a cumulative annual growth rate of 6.8 %.[1] Succinic acid is used as a C4 building block for synthesis of polyesters,[2–4] polyurethane,[5] cosmetics,[6,7] and pharmaceuticals.[8–11] In addition, it is also a precursor to 1,4-butanediol,[12,13] vinyl pyrrolidone,[14] and succinimide.[15] Currently, oil-derived succinic acid is produced by oxidation of butane though maleic anhydride[16–18] or maleic acid[19] intermediates. Other methods involve oxidation of 1,4-butanediol and carbonylation of ethylene glycol.[20] These processes are no longer attractive from the perspective of a sustainable and carbon neutral future. Therefore, alternative means of succinic acid synthesis from biomass is desirable.

The synthesis of succinic acid as a four-carbon chemical from biomass is difficult because of low abundance of tetrose sugars such as erythrose. Until now, bacterial fermentation of hexose sugars with bovine rumen bacteria is the most successful method for synthesis of bio-succinic acid.[21] Although bacterial fermentation provides succinic acid in good selectivity, its industrial application has not been successful due to high operation cost.[22]

Catalytic synthesis of succinic acid from biomass is possible by oxidation of furfural, produced by dehydration of pentoses (xylose and arabinose)[23–26] and hexoses (glucose and fructose). [27–30] Eliminating one carbon atom from furfural through oxidative cleavage of the formyl group to liberate formic acid can produce succinic acid (Scheme 1). Brønsted acid catalysts having an aromatic framework have been reported as catalysts for this reaction. Amberlyst 15, a catalyst with -SO_3H groups on polymeric resin, produces 72 % succinic acid in the presence of aq. H_2O_2.[31,32] A π-π interaction between furfural and the benzene rings of polymeric resin stabilized the furfural during the reaction. Sulphonated graphene oxide, which has a polyaromatic extended 2D π-electron network, showed improved result of 88 % succinic acid yield owing to better interaction with furfural.[33] However, catalyst deactivation due to formation of humins is a major issue in furfural chemistry and catalyst with organic framework cannot be reactivated by calcination to remove organic deposits. Therefore, alternative catalysts should be designed for this reaction.

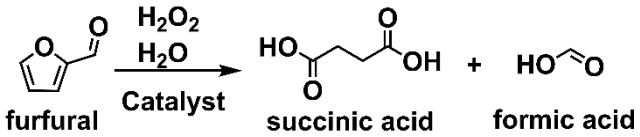

Scheme 1. Catalytic oxidation of furfural to bio-based succinic acid.

Here, we report a different approach to produce succinic acid through Baeyer-Villiger oxidation (BVO) of furfural in the presence of Lewis acid catalysts. Water tolerant zeolites having tetravalent cations like Sn^{4+} and Ti^{4+} in the framework instead of aluminum are known to exhibit pure Lewis acidity.[34] The catalytic property of such zeolites is well studied and they are known to be active for BVO[35,36] and Meerwein–Ponndorf–Verley reduction.[37,38] Among these catalysts, titanium silicalite-1 zeolite (TS−1), has been reported for furfural oxidation to maleic acid in 53 % yield.[39–42] In contrast, we show that Sn containing beta zeolite catalyzes furfural oxidation to succinic acid. In our study, we identify the key intermediate for succinic acid formation and investigate the reasons for high selectivity of Sn-Beta towards succinic acid and propose a reaction mechanism.

Experimental

Catalyst preparation

Sn/Beta catalyst was prepared according to a procedure mentioned elsewhere.[43] In a typical synthesis procedure, 4 g of calcined zeolite (Zeolyst CP814C*, SiO_2/Al_2O_3 = 38, hereafter HBeta-38) was added to 100 mL of 13 N HNO_3 and the solution was refluxed at 100 °C for 20 h. Then the mixture was cooled to room temperature, followed by filtration, and washed with 2 L of deionized water and then dried at 100 °C for 18 h. The resultant dealuminated zeolite was named as DeAl-Beta and 1.5 g of this material was mixed with 0.0562 g of Sn(II) acetate in a mortar. The mixture was ground for 10 min along with scratching with a teflon spatula at regular intervals and then heated under N_2 flow at 500 °C for 3 h, with a ramp rate of 10 °C / min, followed by additional 3 h under air flow. The resulting catalyst was named as 2Sn-Beta with 2 wt. % Sn loading. Catalysts with other Sn loadings were prepared by changing the amount of Sn(II) acetate used. TS-1 was purchased from ACS Material and used without modification. SnO_2 powder was bought from FUJIFILM Wako Pure Chemical Corporation and used as it is.

Catalyst Characterization

X-ray diffraction (XRD) was measured with Rigaku MiniFlex using CuKα X-ray (λ = 1.54 Å) operating at 40 kV and 20 mA. UV-visible diffuse reflectance spectroscopy (UV-vis) measurement was obtained using Jasco V-650 spectrophotometer, line width of light source was kept at 1 nm and polytetrafluoroethylene (PTFE) was used as reference. UV-Vis of liquids samples of 3,3',5,5'-tetramethylbenzidine (TMB) oxidation reaction was carried out in the same instrument, using water as reference. N_2 adsorption isotherms were measured at −196 °C using a Belsorp mini analyzer. Surface area was calculated by using the BET theory in the relative pressure range 0.05 to 0.35 in the N_2 adsorption isotherm.[44] Pyridine IR was done in a Shimadzu IR spirit instrument and the detailed procedure for analysis and quantification of Lewis acid sites is described in supporting information. Diffuse reflectance infrared

Fourier transform spectroscopy (DRIFTS) of furfural adsorption was performed with Perkin Elmer Spectrum 100 instrument. The detailed experimental procedure is described in supporting information.

Catalytic oxidation of Furfural and product analysis

In a typical oxidation reaction, 1 mmol of furfural (distilled before use) was dissolved in 5 mL water in a two neck round bottom flask and 50 mg of catalyst was added. The flask was placed in a preheated oil bath and 44 mmol of H_2O_2 was added and the reaction time was set to zero. After the completion of reaction, the catalyst was separated by centrifugation and washed with acetonitrile to extract the compounds with poor water solubility. An additional wash was performed with water and all the collected liquids were mixed together and diluted to a fixed volume. This solution was analyzed using a Shimadzu HPLC system equipped with a Biorad Aminex HPX-87H column and an RID detector. Quantification was using commercial standards for calibration except for 2(3H)-furanone because it is not commercially available. Instead, its concentration was determined using the calibration factor of 2(5H)-furanone. Furfural conversion (X_F) and product yields (Y_P) were calculated using the following equations.

$$X_F = \frac{N_F\ initial - N_F\ remaining}{N_F\ initial} \times 100\ \%$$

$$Y_P = \frac{N_P\ obtained}{N_F\ initial} \times 100\ \%$$

Where N_F is the number of moles of furfural and N_P is the number of moles of product.

Results and discussion

Catalyst characterization

Sn-Beta catalysts were prepared by dealumination of HBeta-38 to remove Brønsted acid sites followed by inclusion of Sn atoms in the empty T-sites in order to have pure Lewis acid sites. The dealumination and Sn inclusion did not change the surface area and pore volume of the zeolite and the microporous structure was intact (Figure S1 and Table S1). Nature of acid sites in the prepared catalysts was analyzed by pyridine

adsorption IR experiment to study the change in Brønsted and Lewis acid density (Figure 1a). After pyridine adsorption, the peak at 1455 cm^{-1} was assigned to ring vibration of coordinatively bound surface pyridine species to Lewis acid sites and the peak at 1540 cm^{-1} was assigned to that of surface pyridinium ions interacting with Brønsted acid sites.[45] Lewis acid density of 2Sn-Beta (containing 2 wt. % Sn loading) was higher than the parent HBeta-38 zeolite, whereas the Brønsted acid density was negligible. The Brønsted acid sites were lost during dealumination of HBeta-38 because the charge imbalance between tetravalent Si and trivalent Al was no longer present. Sn itself being tetravalent leads to an electrically neutral framework, hence there is no proton as counter balancing ion to generate Brønsted acidity in the 2Sn-Beta catalyst. DeAl-Beta showed no acidity and the peaks at 1445 and 1435 cm^{-1} were assigned to hydrogen bonding interaction with pyridine, probably because of high number of silanol groups. Hence, it can be concluded that Lewis acidity in the 2Sn-Beta catalyst was due to Sn incorporation.

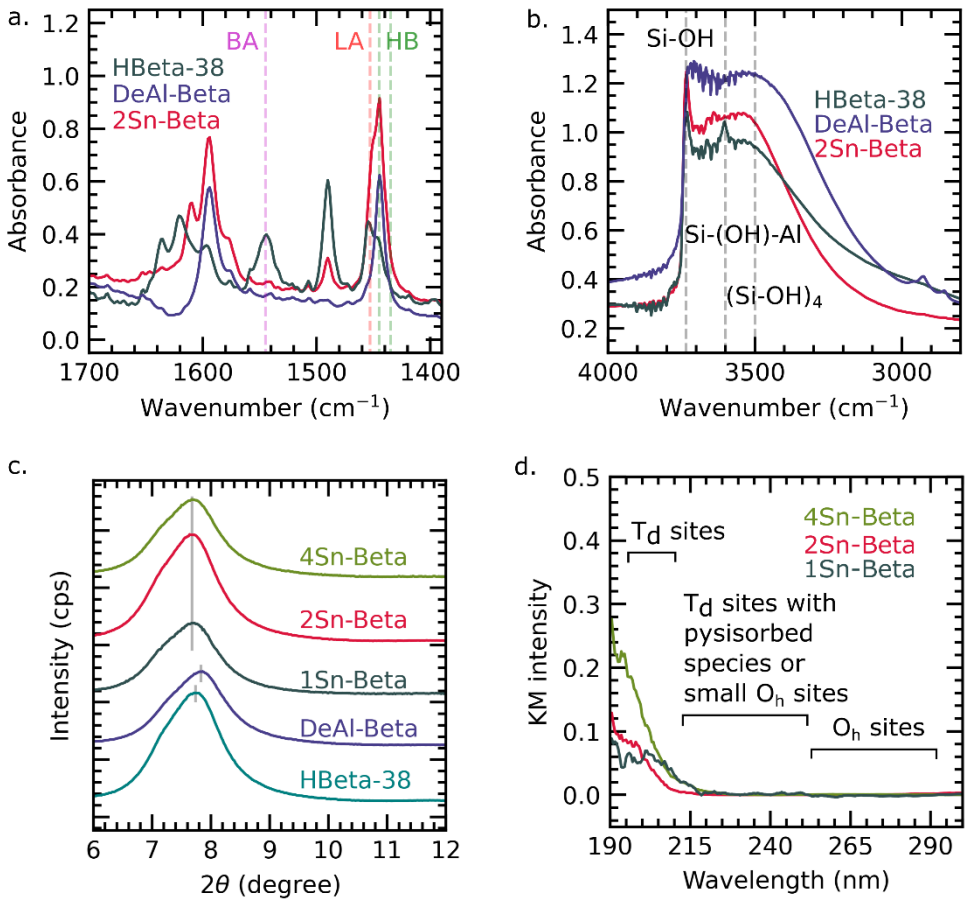

Figure 1. a) Pyridine adsorption IR spectrum for HBeta-38, DeAl-Beta and 2Sn-Beta. BA, LA and HB indicate peaks due to Brønsted acidity, Lewis acidity and hydrogen bonded pyridine, respectively. b) Normalized IR spectrum of silanol region showing dealumination and Sn incorporation into zeolite Beta. c) XRD of various catalysts. d) UV-Visible spectrum of Sn-Beta with different Sn loading.

The dealumination and Sn incorporation process was also monitored by FTIR analysis of the silanol region (Figure 1b). Spectrum for HBeta-38 consisted of two sharp peaks at 3710 cm^{-1} and 3600 cm^{-1} that were assigned to -OH stretching of individual surface terminated silanol groups (Si-OH)[46] and -OH stretching of bridged -OH groups between neighboring Si and Al, respectively. A broad peak with relatively less intensity ranging from 3200 to 3600 cm^{-1} was assigned to hydrogen bonded silanol nests.[46] After dealumination the -OH stretching of bridged -OH groups at 3600 cm^{-1} disappeared as Si-O-Al bridges were no longer present. Simultaneously, the relative intensity of the broad peak increased due to creation of new hydrogen bonded silanol nests. These silanol nests serve as anchoring site for the incoming Sn cations. After incorporation of Sn, the relative intensity of the broad peak decreased in comparison to terminated -OH stretching peak at 3710 cm^{-1} because some of the nests were now occupied with Sn atoms.

The dealumination and Sn incorporation also caused a change in the lattice structure of zeolite, which was observed by powder XRD of the catalysts. The diffraction peak of zeolite crystal at $2\theta = 7.8°$ shifted to higher 2θ value after dealumination (Figure 1c), which was attributed to lattice shrinkage due to removal of Al atoms from the HBeta-38 unit cell.[47] The peak position shifted back to lower 2θ after incorporation of Sn. Moreover, diffraction peaks for SnO_2 were not observed in XRD even when Sn loading was increased to 4 wt. % (Figure S2). SnO_2 can form due to oligomerization of Sn species that are unable to form a tetrahedrally coordinated Sn site in the empty silanol nests. The absence of diffraction for SnO_2 could either mean that there are no SnO_2 particles or that the SnO_2 particles are small and lack long range order.

Further insight into SnO_2 formation was obtained by observing the shift in UV-visible absorption maxima with respect of Sn loading in Sn-Beta catalyst. The shift in absorption maxima can be correlated with Sn coordination number and particle size domain.[48–50] 1Sn Beta, 2Sn-Beta and 4Sn-Beta catalysts, having 1,2 and 4 wt. % Sn content, only showed absorption below 215 nm assigned to isolated tetrahedral Sn atoms (T_d) of Sn-Beta zeolite (Figure 1d).[51] Therefore, all the catalysts had Sn exclusively present as Lewis acidic tetrahedral Sn sites.

Furfural oxidation over different catalysts

Furfural oxidation in water and H_2O_2 in the absence of any catalyst showed 5 % succinic acid yield along with slight amount of 2(5H)-furanone (Figure 2). In the presence of 2Sn-Beta, under optimized condition the yield of succinic acid was 53 % (reaction optimization data is shown in Figure S3). Maleic acid, malic acid and 2(5H)-furanone were the major by-products. HBeta-38 catalyst was not selective and produced comparable amounts of succinic acid, 2(5H)-furanone and maleic acid. Activity of pure SnO_2 was not much different from HBeta-38, which shows that pure Lewis acidic nature of Sn is important for succinic acid selectivity. In contrast, another Lewis acid zeolite TS-1 produced maleic acid selectively with low amount of succinic acid. This behavior of TS-1 is consistent with previous reports describing selective synthesis of maleic acid.[39–42] From these results it is evident that while Brønsted acid zeolite was not selective towards any product, Lewis acid catalysts (Sn-Beta and TS-1) were able to selectively produce succinic acid or maleic acid. Formic acid was formed as the secondary product in all cases due to oxidative cleavage of the formyl group, irrespective of the catalyst used. The recyclability of 2Sn-Beta was investigated, and the catalyst activity did not drop for four catalytic cycles (Figure S4). However, after four cycles the color of the catalyst changed from white to pale yellow, suggesting deposition of organic matter on the catalyst. Calcining the catalyst at 550 °C for 3 h removed the organic deposit and recovered white color of the catalyst. The recalcined catalyst showed no loss of activity. This shows that the catalyst was not prone to deactivation and deposited organic matter can be removed by calcination without any loss of activity.

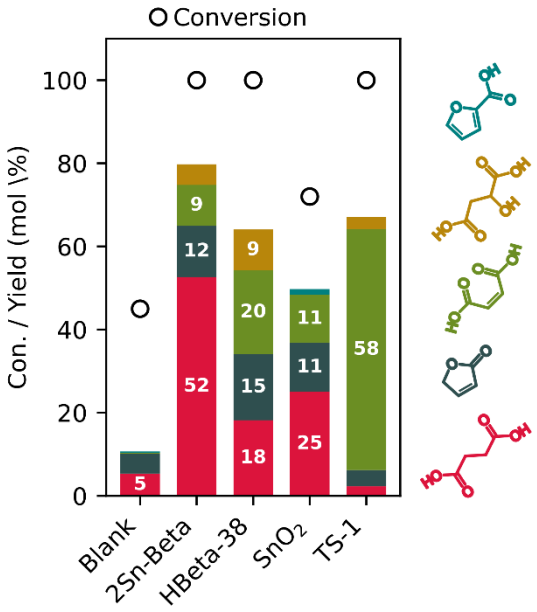

Figure 2. Catalytic activity of different catalysts for furfural oxidation reaction. Reaction conditions: furfural 1 mmol (96 mg), catalyst 50 mg, 15 % H_2O_2 solution 10 mL, 50 °C, 6 h.

The time course of reaction in the presence of 2Sn-Beta showed that the formation of succinic acid was preceded by formation of 2(3H)-furanone (Figure 3a). This compound has been suggested as an intermediate in earlier studies.[31,32] We were able to positively identify 2(3H)-furanone by NMR (Figure S5-6) and mass spectrometry (Figure S7-8) of product solution and quantified it using LC (see Figure S9 for typical HPLC profile of furfural oxidation reaction). In contrast to 2Sn-Beta, the formation of 2(3H)-furanone over HBeta-38 was not prominent. In the presence of TS-1, 5-hydroxy-2(3H)-furanone was formed as the major intermediate for maleic acid. Some byproducts were formed in the presence of all three catalysts. The carbon balance for 2Sn-Beta and TS-1 catalyst was stable after 60 mins of reaction, which indicates that most of the unidentified byproducts were formed by side reaction of furfural during the initial phase of the reaction. (Figure S10)

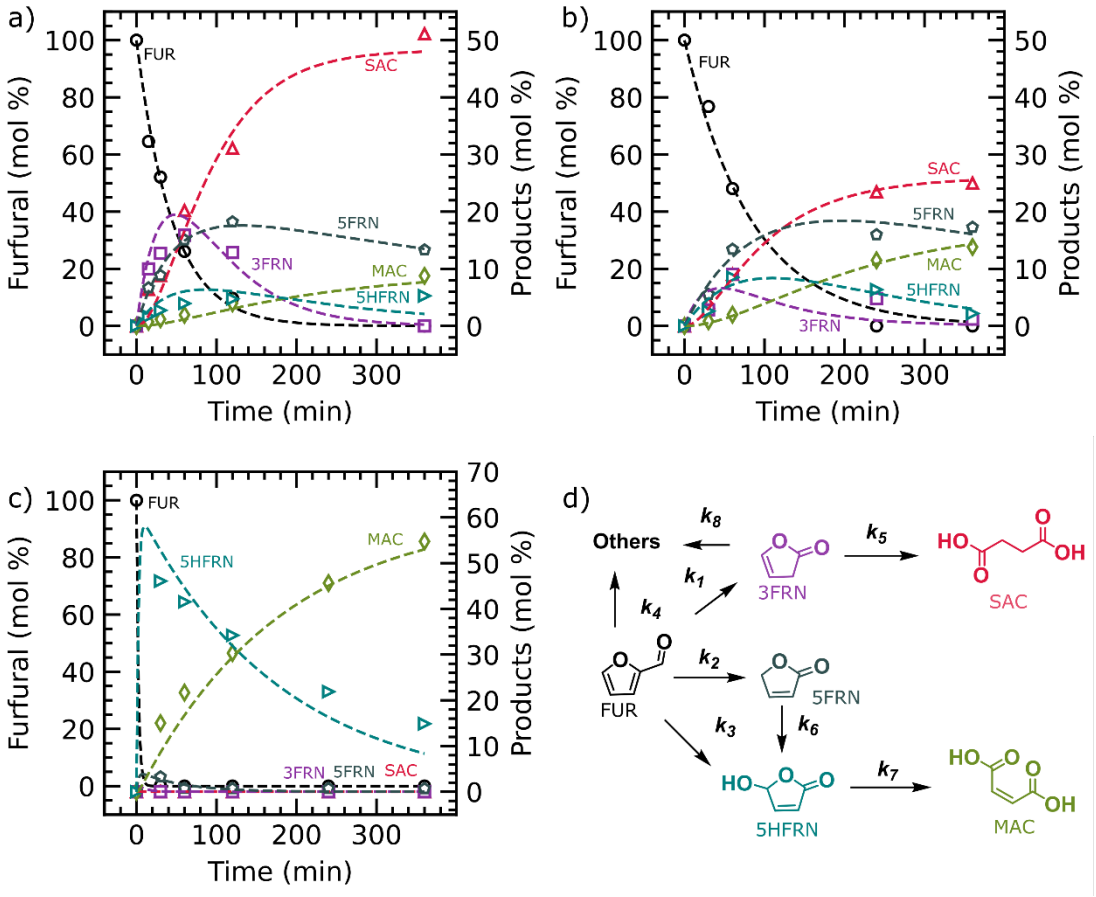

Figure 3. Time course of furfural oxidation in the presence of (a) 2Sn-Beta, (b) HBeta-38 and (c) TS-1. The symbols represent experimental data and the lines show fitting of experimental data with reaction model shown in (d). Reaction conditions: furfural 1 mmol (96 mg), catalyst 50 mg, 15 % H_2O_2 solution 10 mL, 50 °C

We performed kinetic analysis of the reaction by using reaction scheme shown in Figure 3d and modelling the experimental data using equations 1-6.

$$\frac{d[FUR]}{dt} = -(k_1 + k_2 + k_3 + k_4) \times [FUR] \quad (1)$$

$$\frac{d[3FRN]}{dt} = k_1[FUR] - (k_5 + k_8) \times [3FRN] \quad (2)$$

$$\frac{d[5FRN]}{dt} = k_2 \times [FUR] - k_6 \times [5FRN] \quad (3)$$

$$\frac{d[5HFRN]}{dt} = k_3 \times [FUR] + k_6 \times [5FRN] - k_7 \times [5HFRN] \quad (4)$$

$$\frac{d[SAC]}{dt} = k_5 \times [3FRN] \quad (5)$$

$$\frac{d[MAC]}{dt} = k_7 \times [5HFRN] \quad (6)$$

where k_1-k_7 represent rate constants for reactions shown in Figure 3d, FUR stands for furfural, 3FRN for 2(3H)-furanone, 5FRN for 2(5H)-furanone, 5HFRN for 5-hydroxy-2(5H)-furanone, SAC for succinic acid and MAC for maleic acid. Products like furoic acid and malic acid were not modeled in the reaction as their concentration was too low during reaction.

Rate constants were estimated by fitting the model to experimental data by assuming pseudo-first order-reactions (Table 1). The formation rates of 2(3H)-furanone (k_1 = 0.64 h^{-1}) and 2(5H)-furanone (k_2 = 0.28 h^{-1}) were higher in the presence of 2Sn-Beta catalyst in comparison to other reaction pathways. Whereas, in the case of Brønsted acid containing HBeta-38, both 2(3H)-furanone and 2(5H)-furanone had similar formation rates. Moreover, the rates of formation for 5-hydroxy-2(3H)-furanone (k_3) and furfural degradation (k_4) were also comparable to the hydrofuranone formation rates, which was the reason for nonselective reaction. The kinetic analysis of reaction in the presence of TS-1 catalyst showed that formation of 5-hydroxy-2(5H)-furanone was highly favored. This is why TS-1 selectively produced maleic acid. Therefore, it is evident that higher rate of formation of 2(3H)-furanone over Lewis acidic 2Sn-Beta was the primary reason for selective succinic acid formation. Moreover, the subsequent conversion of 2(3H)-furanone to succinic acid was faster than its formation from furfural ($k_5 > k_1$). The formation of 2(3H)-furanone is possible via BVO of furfural as shown in Scheme 2. BVO of furfural would produce a formate ester which would undergo hydrolysis in the presence of water to yield a furan alcohol. The isomerization of furan alcohol would produce 2(3H)-furanone and 2(5H)-furanone.

Table 1. Estimated rate constants from the kinetic fitting. The rate constants are in the unit of h^{-1}.

Catalyst	k_1	k_2	k_3	k_4	k_5	k_6	k_7	k_8
2Sn-Beta	0.64	0.28	0.13	0.28	1.12	0.09	0.30	0
HBeta-38	0.24	0.18	0.13	0.17	1.63	0.09	0.41	0.48
TS-1	-	-	12.5	6.67	-	-	0.33	-

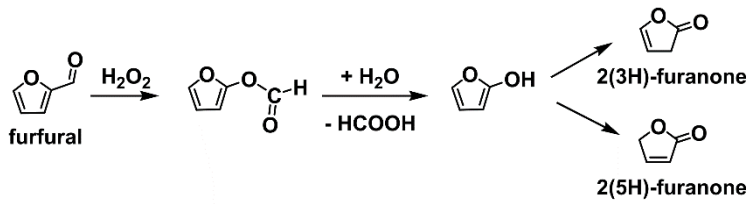

Scheme 2. Formation pathway of hydrofuranones from furfural.

The BVO reaction of aldehydes is catalyzed by Lewis acid sites.[52,53] Therefore, we investigated the influence of Lewis acid density of Sn-Beta catalysts for furfural oxidation. The Lewis acid density was calculated by quantitative analysis after pyridine adsorption IR spectra of catalysts with different Sn loading. The peak intensity of adsorbed pyridine at 1455 cm^{-1} increased steadily with increase in Sn loading (Figure 4a). The initial catalytic activity (expressed as sum of moles of succinic acid and 2(3H)-furanone per hour) increased with the Lewis acid density (Figure 4b). This indicates that activation of furfural over Lewis acidic Sn sites followed by BVO was important for higher selectivity.

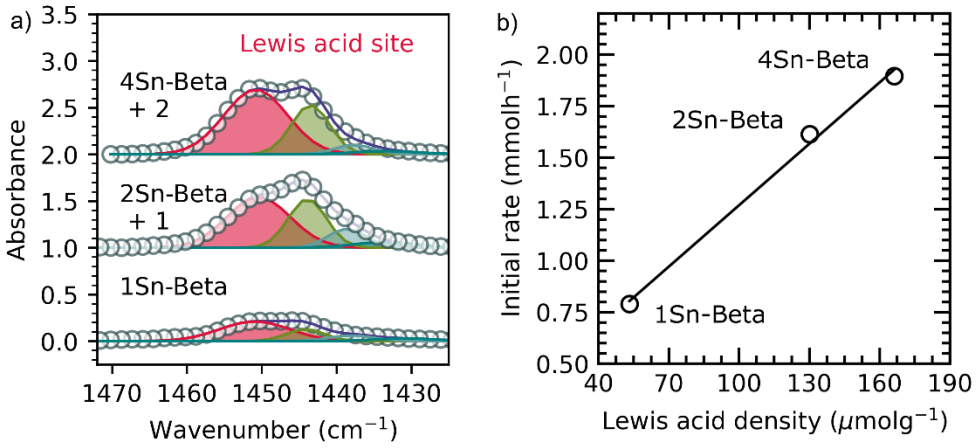

Figure 4. (a) Deconvoluted pyridine adsorption IR spectrum of Sn-Beta catalysts in the Lewis acid region, the crimson color peak at 1455 cm^{-1} represents ring vibration of pyridine interacting with Lewis acid sites, other peaks correspond to ring vibration of hydrogen bonded pyridine to silanol groups, line with blue markers represents experimental data. (b) Plot of Lewis acid site (LAS) density vs initial activity. Reaction conditions: furfural 5 mmol (480 mg), catalyst 50 mg, 15 % H_2O_2 solution 10 mL, 50 °C, 1 h.

In order to investigate the role of Sn-Beta in promoting BVO reaction we observed the interaction of catalyst with furfural and H_2O_2. Diffused reflectance infrared Fourier transform spectroscopy (DRIFTS) experiment was performed to observe the activation of furfural over 2Sn-Beta. Prior to DRIFTS analysis, the catalyst surface was saturated with furfural and then excess furfural was desorbed by heating under vacuum. DRIFTS analysis of adsorbed furfural on 2Sn-Beta catalyst showed two peaks at 1724 cm^{-1} and 1671 cm^{-1} in the carbonyl region (Figure 5). The first peak was assigned to carbonyl stretching frequency of uncoordinated furfural and second one to furfural coordinated with a strong Lewis acid site. A shoulder peak to the 1671 cm^{-1} appeared at 1690 cm^{-1}, which can be assigned to furfural coordinated to a possible weak Lewis acidic site on the catalyst. From this observation it can be inferred that Sn sites of Sn-Beta strongly interacted with the carbonyl group of furfural. Similar interaction was not observed for the parent zeolite HBeta-38 in which Brønsted acid sites are dominant species compared to Lewis acid sites. On the other hand, TS-1 showed a weaker adsorption of furfural carbonyl group in comparison to 2Sn-Beta. The

redshift in carbonyl peak position was less severe at 1687 cm^{-1} for TS-1. Therefore, we can conclude that 2Sn-Beta strongly adsorbed the carbonyl group of furfural and adsorption on TS-1 was weaker. When coordinated to the Lewis acid sites, electrophilicity of the carbonyl carbon atom increases and from the above observations 2Sn-Beta was most effective in this regard.

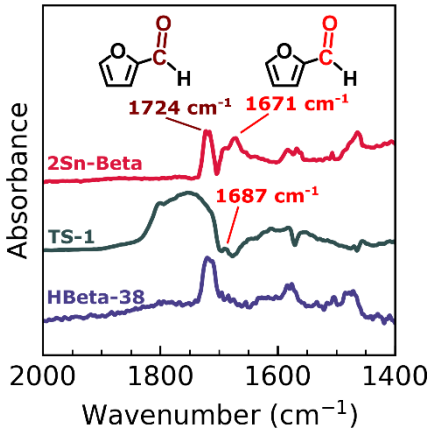

Figure 5. DRIFTS spectra of furfural adsorbed on various catalysts.

The interaction of catalysts with H_2O_2 is also a major factor that influences selectivity. Activation of H_2O_2 may produce species that are even stronger nucleophiles in comparison to H_2O_2. We treated the catalysts with aqueous H_2O_2 solution and observed the diffuse reflectance UV-visible spectra. H_2O_2 is activated on the surface of the catalyst to form metal-hydroperoxy (M-OOH) species, which gives rise to a yellow color, and it appears as a peak around 390 nm in UV-vis (Figure 6). Only TS-1 showed activity for formation of Ti-OOH species and both 2Sn-Beta and HBeta-38 zeolite were inactive. Formation of Ti-OOH species with TS-1 in the presence of H_2O_2 is consistent with literature.[54,55] At this point it is worth mentioning that metal hydroperoxy species are known to catalyze the epoxidation reaction; hence the formation of 5-hydroxy-2(5H)-furanone over TS-1 could be a direct result of epoxidation of the double bond between C4-C5 carbon atoms of furfural in the presence of Ti-OOH species (Scheme S1).

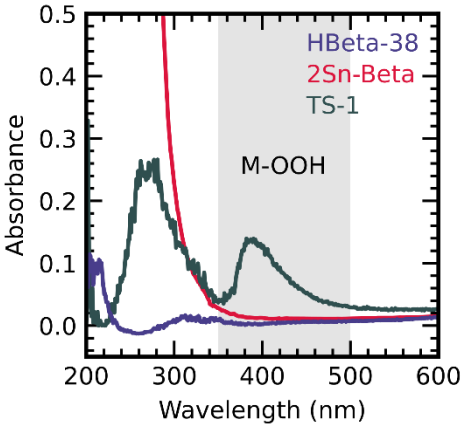

Figure 6. UV-vis spectroscopy of catalysts showing formation of M-OOH species in the presence of H_2O_2 on TS-1.

In addition to surface activation, H_2O_2 can also be activated in solution. The activation of H_2O_2 with HBeta-38 was tested by two-electron oxidation of 3,3',5,5'-tetramethylbenzidine (TMB), shown in Figure 7a.[56–58] The oxidation product is a blue color compound, which can be monitored with UV-visible spectrum. The activity of 2Sn-Beta for oxidation of TMB was quite low and almost no reaction occurred after 30 min (Figure 7b), which shows 2Sn-Beta has limited ability to activate H_2O_2 in solution. On the other hand, in the presence of HBeta-38, rapid oxidation of TMB proceeded, which implies that H_2O_2 was activated by HBeta-38, probably via protonation of H_2O_2. The UV-Visible spectra of reaction mixtures at 35 minutes is shown in the supporting information (Figure S11). This leads to the conclusion that pure Lewis acid nature of Sn-Beta catalyst is important for formation of succinic acid.

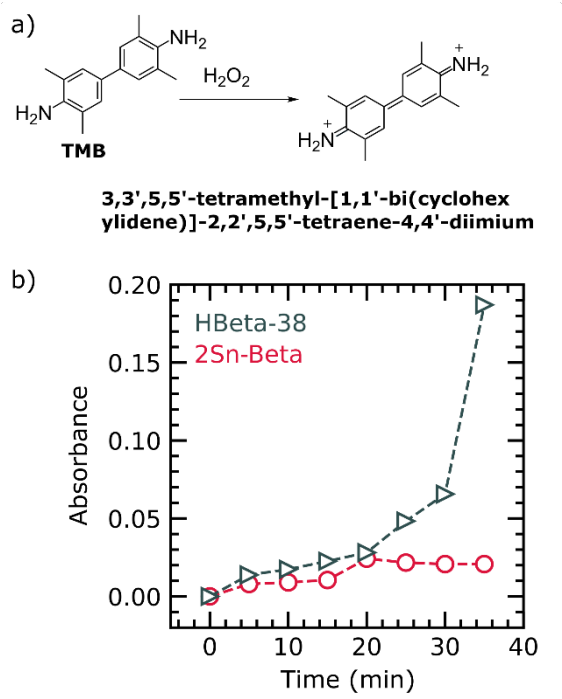

Figure 7. Evolution of TMB oxidation product with time monitored using UV-Vis spectroscopy. (a) TMB oxidation reaction scheme. (b) Time-course of band centered around 660 nm in UV-Vis spectra of TMB oxidation reaction in the presence of HBeta-38 and 2Sn-Beta.

From the above observations, it can be summarized that 2Sn-Beta does not interact with H_2O_2 either to form M-OOH or to activate H_2O_2 in solution. In contrast, TS-1 makes surface hydroperoxy species and HBeta-38 activates H_2O_2 via protonation.

Considering the strong adsorption of furfural on Lewis acid sites of 2Sn-Beta catalyst and the lack of interaction between H_2O_2 and catalyst, we propose the following reaction mechanism for succinic acid formation (Scheme 3). Furfural is first adsorbed on the tetrahedrally coordinated Sn site of Sn-Beta, which polarizes the C=O bond to make the carbon more electron deficient. A nucleophilic attack of H_2O_2 on the electron deficient carbonyl carbon forms formate easter via Baeyer-Villiger oxidation, followed by hydrolysis to form a furan alcohol. Keto-enol tautomerization of the furan alcohol produces 2(3H)-furanone and 2(5H)-furanone. While 2(5H)-furanone is stable, 2(3H)-furanone undergoes hydrolysis with oxidative ring opening to form a succinic semialdehyde. This compound is not stable in aqueous solution and undergoes oxidation to form succinic acid.

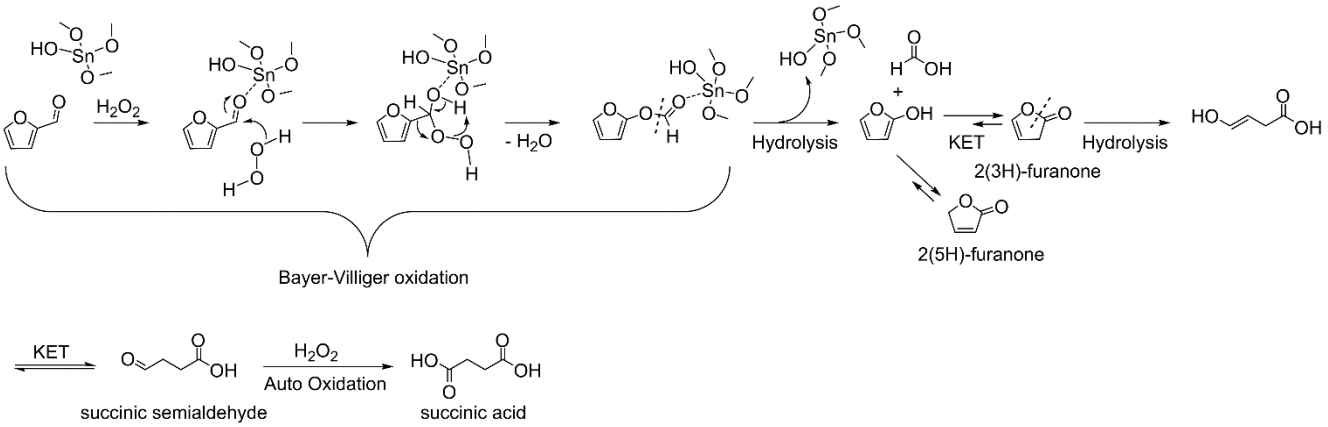

Scheme 3. Proposed reaction pathway for furfural oxidation to succinic acid over Sn-Beta Lewis acid catalyst.

Lastly, it is crucial to understand the role of formic acid, formed in situ, as a Brønsted acid catalyst during the reaction. Formic acid alone, when added externally (1 mmol), at the start of the reaction resulted in higher furfural conversion and succinic acid yield in comparison to a non-catalytic reaction (Figure S12). Therefore, formic acid alone does work as a Brønsted acid catalyst to promote the oxidation reaction. However, furfural conversion and succinic acid selectivity in the presence of formic acid was lower than 2Sn-Beta catalyst. The Brønsted acidity of formic acid might also influence the latter steps of the reaction. To investigate this, we prepared a mixture of 2(3H)-furanone and 2(5H)-furanone and used it as the reactant. Under all conditions 2(3H)-furanone was completely consumed. However, maximum yield of succinic acid was only obtained in the presence 2Sn-Beta and use of formic acid reduced the succinic acid yield (Table S2). Therefore, it can be argued that while formation of formic acid does influence the reaction, Lewis acidic Sn-Beta catalyst was responsible for higher succinic acid selectivity.

Conclusion

In conclusion, we have shown that furfural oxidation with pure Lewis acidic Sn-Beta forms succinic acid with a yield of 53 %. 2(3H)-Furanone was identified as the intermediate for succinic acid formation and kinetic analysis showed that its formation by Baeyer-Villiger oxidation was promoted over Sn-Beta catalyst.

The rate of reaction was directly correlated with the density of Lewis acid sites, which activated the aldehyde group of furfural as observed in DRIFTS analysis. In addition, the inability of Sn-Beta to activate H_2O_2 suppressed the side reactions to achieve a high succinic acid selectivity. In contract, furfural oxidation reaction over HBeta-38 and TS-1 was not selective because they activated H_2O_2 either in solution form or as metal hydroperoxy species. The Sn-Beta catalyst was reusable for several cycles and organic deposits were easily removed by recalcination without any loss in catalytic activity. Consequently, we show that Sn-Beta is a unique and reusable Lewis acid catalyst for furfural oxidation to succinic acid.

Supporting Information

The Supporting Information is available free of charge at https://pubs.acs.org/doi/10.1021/xxx

Additional catalyst characterization, reaction optimization, catalyst recyclability, detailed identification of key intermediates, procedure for TMB oxidation reaction, reactions with formic acid as catalyst.

Author information

Corresponding Authors

Abhijit Shrotri - Institute for Catalysis, Hokkaido University, Kita 21 Nishi 10, Kita-ku, Sapporo, Hokkaido 001-0021, Japan; orcid.org/0000-0001-9850-7325; Email: ashrotri@cat.hokudai.ac.jp

Atsushi Fukuoka - Institute for Catalysis, Hokkaido University, Kita 21 Nishi 10, Kita-ku, Sapporo, Hokkaido 001-0021, Japan; orcid.org/0000-0002-8468-7721; Email: fukuoka@cat.hokudai.ac.jp

Authors

Yayati Naresh Palai - Institute for Catalysis, Hokkaido University, Kita 21 Nishi 10, Kita-ku, Sapporo, Hokkaido 001-0021, Japan. Graduate School of Chemical Sciences and Engineering, Hokkaido University, Kita 13 Nishi 8, Kita-ku, Sapporo, Hokkaido 060-8628, Japan.

Notes

The authors declare no competing financial interest.

Acknowledgement

This work was supported by JSPS KAKENHI Grant Number JP21H01708.

References

(1) Markets and Markets. Succinic Acid Market by Type (Bio-Based Succinic Acid, Petro-Based Succinic Acid), End-Use Industry (Industrial, Food & Beverage, Coatings, Pharmaceutical), and Region (APAC, Europe, North America, South America, Middle East & Africa) - Forecast to 2023 https://www.marketsandmarkets.com/Market-Reports/succinic-acid-market-402.html (accessed Sep 6, 2021).

(2) Harmsen, P. F. H.; Hackmann, M. M.; Bos, H. L. Green Building Blocks for Bio-based Plastics. *Biofuels, Bioprod. Biorefining* **2014**, *8* (3), 306–324.

(3) Luman, N. R.; Kim, T.; Grinstaff, M. W. Dendritic Polymers Composed of Glycerol and Succinic Acid: Synthetic Methodologies and Medical Applications. *Pure Appl. Chem.* **2004**, *76* (7–8), 1375–1385.

(4) Sacan, L.; Cirpan, A.; Camurlu, P.; Toppare, L. Conducting Polymers of Succinic Acid Bis-(2-Thiophen-3-Yl-Ethyl) Ester and Their Electrochromic Properties. *Synth. Met.* **2006**, *156* (2–4), 190–195.

(5) Sonnenschein, M. F.; Guillaudeu, S. J.; Landes, B. G.; Wendt, B. L. Comparison of adipate and succinate polyesters in thermoplastic polyurethanes. *Polymer* **2010**, *51* (16), 3685–3692.

(6) Tashiro, M.; Nagare, Y.; Matsui, T. Oil-in-Water Emulsion Cosmetic. US 2020/0155440 A1, May 21, 2020.

(7) Sarosi, C.; Moldovan, M.; Miuta, F.; Prodan, D.; Antoniac, A.; Prejmerean, C.; Silaghi Dumitrescu, L.; Popescu, V.; Raiciu, A. D.; Saceleanu, V. Preparation and Characterization of Natural Bleaching Gels Used in Cosmetic Dentistry. *Materials* **2019**, *12* (13), 2106.

(8) Pfister, B.; Jonsson, J.; Gustafsson, M. Drug-Related Problems and Medication Reviews among Old People with Dementia. *BMC Pharmacol. Toxicol.* **2017**, *18* (1), 52.

(9) Zhang, F.; Zhou, F.; Wei, W. Comparison the Effect of Shengxuening Tablets and Ferrous Succinate in Treating Pregnancy with Anemia. *Chinese J. Biochem. Pharm.* **2017**, *37* (2), 68–71.

(10) Plumb, D. C. *Plumb's Veterinary Drug Handbook: Desk*; John Wiley & Sons, 2018.

(11) Cao, G.-Y.; Li, K.-X.; Jin, P.-F.; Yue, X.-Y.; Yang, C.; Hu, X. Comparative Bioavailability of Ferrous Succinate Tablet Formulations without Correction for Baseline Circadian Changes in Iron Concentration in

Healthy Chinese Male Subjects: A Single-Dose, Randomized, 2-Period Crossover Study. *Clin. Ther.* **2011**, *33* (12), 2054–2059.

(12) Ly, B. K.; Minh, D. P.; Pinel, C.; Besson, M.; Tapin, B.; Epron, F.; Especel, C. Effect of Addition Mode of Re in Bimetallic Pd–Re/TiO 2 Catalysts upon the Selective Aqueous-Phase Hydrogenation of Succinic Acid to 1, 4-Butanediol. *Top. Catal.* **2012**, *55* (7–10), 466–473.

(13) Minh, D. P.; Besson, M.; Pinel, C.; Fuertes, P.; Petitjean, C. Aqueous-Phase Hydrogenation of Biomass-Based Succinic Acid to 1, 4-Butanediol over Supported Bimetallic Catalysts. *Top. Catal.* **2010**, *53* (15–18), 1270–1273.

(14) Haus, M. O.; Louven, Y.; Palkovits, R. Extending the Chemical Product Tree: A Novel Value Chain for the Production of N-Vinyl-2-Pyrrolidones from Biogenic Acids. *Green Chem.* **2019**, *21* (23), 6268–6276.

(15) Liu, Y.; Fu, J.; Ren, D.; Song, Z.; Jin, F.; Huo, Z. Efficient Synthesis of Succinimide from Succinic Anhydride in Water over Unsupported Nanoporous Nickel Material. *ChemistrySelect* **2018**, *3* (2), 724–728.

(16) Huang, Y.; Ma, Y.; Cheng, Y.; Wang, L.; Li, X. Active Ruthenium Catalysts Prepared by Cacumen Platycladi Leaf Extract for Selective Hydrogenation of Maleic Anhydride. *Appl. Catal. A Gen.* **2015**, *495*, 124–130.

(17) Liao, X.; Zhang, Y.; Hill, M.; Xia, X.; Zhao, Y.; Jiang, Z. Highly Efficient Ni/CeO2 Catalyst for the Liquid Phase Hydrogenation of Maleic Anhydride. *Appl. Catal. A Gen.* **2014**, *488*, 256–264.

(18) Torres, C. C.; Alderete, J. B.; Mella, C.; Pawelec, B. Maleic Anhydride Hydrogenation to Succinic Anhydride over Mesoporous Ni/TiO_2 Catalysts: Effects of Ni Loading and Temperature. *J. Mol. Catal. A Chem.* **2016**, *423*, 441–448.

(19) Granados, M. L.; Moreno, J.; Alba-Rubio, A. C.; Iglesias, J.; Alonso, D. M.; Mariscal, R. Catalytic Transfer Hydrogenation of Maleic Acid with Stoichiometric Amounts of Formic Acid in Aqueous Phase: Paving the Way for More Sustainable Succinic Acid Production. *Green Chem.* **2020**, *22* (6), 1859–1872.

(20) Cornils, B.; Lappe, P.; by Staff, U. Dicarboxylic Acids, Aliphatic. *Ullmann's Encycl. Ind. Chem.* **2014**, 1–18.

(21) Song, H.; Lee, S. Y. Production of Succinic Acid by Bacterial Fermentation. *Enzyme Microb. Technol.* **2006**, *39* (3), 352–361.

(22) Li, X.; Mupondwa, E. Empirical Analysis of Large-Scale Bio-Succinic Acid Commercialization from a Technoeconomic and Innovation Value Chain Perspective: BioAmber Biorefinery Case Study in Canada. *Renew. Sustain. Energy Rev.* **2021**, *137*, 110587.

(23) Wang, Y.; Yang, X.; Zheng, H.; Li, X.; Zhu, Y.; Li, Y. Mechanistic Insights on Catalytic Conversion Fructose to Furfural on Beta Zeolite via Selective Carbon-Carbon Bond Cleavage. *Mol. Catal.* **2019**, *463*, 130–139.

(24) Wang, L.; Guo, H.; Xie, Q.; Wang, J.; Hou, B.; Jia, L.; Cui, J.; Li, D. Conversion of Fructose into Furfural or 5-Hydroxymethylfurfural over HY Zeolites Selectively in γ-Butyrolactone. *Appl. Catal. A Gen.* **2019**, *572*, 51–60.

(25) Wang, Y.; Ding, G.; Yang, X.; Zheng, H.; Zhu, Y.; Li, Y. Selectively Convert Fructose to Furfural or Hydroxymethylfurfural on Beta Zeolite: The Manipulation of Solvent Effects. *Appl. Catal. B Environ.* **2018**, *235*, 150–157.

(26) Asakawa, M.; Shrotri, A.; Kobayashi, H.; Fukuoka, A. Solvent Basicity Controlled Deformylation for the Formation of Furfural from Glucose and Fructose. *Green Chem.* **2019**, *21* (22), 6146–6153.

(27) Gupta, N. K.; Fukuoka, A.; Nakajima, K. Metal-Free and Selective Oxidation of Furfural to Furoic Acid with an N-Heterocyclic Carbene Catalyst. *ACS Sustain. Chem. Eng.* **2018**, *6* (3), 3434–3442.

(28) Gupta, N. K.; Fukuoka, A.; Nakajima, K. Amorphous Nb_2O_5 as a Selective and Reusable Catalyst for Furfural Production from Xylose in Biphasic Water and Toluene. *ACS Catal.* **2017**, *7* (4), 2430–2436.

(29) Lam, E.; Chong, J. H.; Majid, E.; Liu, Y.; Hrapovic, S.; Leung, A. C. W.; Luong, J. H. T. Carbocatalytic Dehydration of Xylose to Furfural in Water. *Carbon* **2012**, *50* (3), 1033–1043.

(30) Dias, A. S.; Pillinger, M.; Valente, A. A. Dehydration of Xylose into Furfural over Micro-Mesoporous Sulfonic Acid Catalysts. *J. Catal.* **2005**, *229* (2), 414–423.

(31) Choudhary, H.; Nishimura, S.; Ebitani, K. Metal-Free Oxidative Synthesis of Succinic Acid from Biomass-Derived Furan Compounds Using a Solid Acid Catalyst with Hydrogen Peroxide. *Appl. Catal. A Gen.* **2013**, *458*, 55–62.

(32) Choudhary, H.; Nishimura, S.; Ebitani, K. Highly Efficient Aqueous Oxidation of Furfural to Succinic Acid Using Reusable Heterogeneous Acid Catalyst with Hydrogen Peroxide. *Chem. Lett.* **2012**, *41* (4), 409–411.

(33) Zhu, W.; Tao, F.; Chen, S.; Li, M.; Yang, Y.; Lv, G. Efficient Oxidative Transformation of Furfural into Succinic Acid over Acidic Metal-Free Graphene Oxide. *ACS Sustain. Chem. Eng.* **2019**, *7* (1), 296–305.

(34) Wolf, P.; Hammond, C.; Conrad, S.; Hermans, I. Post-Synthetic Preparation of Sn-, Ti- and Zr-Beta: A Facile Route to Water Tolerant, Highly Active Lewis Acidic Zeolites. *Dalton Trans.* **2014**, *43* (11), 4514–4519.

(35) Renz, M.; Blasco, T.; Corma, A.; Fornes, V.; Jensen, R.; Nemeth, L. Selective and Shape-Selective Baeyer-

Villiger Oxidations of Aromatic Aldehydes and Cyclic Ketones with Sn-Beta Zeolites and H_2O_2. *Chem. Eur. J.* **2002**, *8* (20), 4708–4717.

(36) Corma, A.; Nemeth, L. T.; Renz, M.; Valencia, S. Sn-Zeolite Beta as a Heterogeneous Chemoselective Catalyst for Baeyer-Villiger Oxidations. *Nature* **2001**, *412* (6845), 423–425.

(37) Corma, A.; Domine, M. E.; Nemeth, L.; Valencia, S. Al-Free Sn-Beta Zeolite as a Catalyst for the Selective Reduction of Carbonyl Compounds (Meerwein-Ponndorf-Verley Reaction). *J. Am. Chem. Soc.* **2002**, *124* (13), 3194–3195.

(38) Corma, A.; Domine, M. E.; Valencia, S. Water-Resistant Solid Lewis Acid Catalysts: Meerwein-Ponndorf-Verley and Oppenauer Reactions Catalyzed by Tin-Beta Zeolite. *J. Catal.* **2003**, *215* (2), 294–304.

(39) Alonso-Fagúndez, N.; Agirrezabal-Telleria, I.; Arias, P. L.; Fierro, J. L. G.; Mariscal, R.; Granados, M. L. Aqueous-Phase Catalytic Oxidation of Furfural with H_2O_2: High Yield of Maleic Acid by Using Titanium Silicalite-1. *RSC Adv.* **2014**, *4* (98), 54960–54972.

(40) Lou, Y.; Marinkovic, S.; Estrine, B.; Qiang, W.; Enderlin, G. Oxidation of Furfural and Furan Derivatives to Maleic Acid in the Presence of a Simple Catalyst System Based on Acetic Acid and TS-1 and Hydrogen Peroxide. *ACS Omega* **2020**, *5* (6), 2561–2568.

(41) Rodenas, Y.; Mariscal, R.; Fierro, J. L. G.; Martín Alonso, D.; Dumesic, J. A.; López Granados, M. Improving the Production of Maleic Acid from Biomass: TS-1 Catalysed Aqueous Phase Oxidation of Furfural in the Presence of γ-Valerolactone. *Green Chem.* **2018**, *20* (12), 2845–2856.

(42) Rodenas, Y.; Fierro, J. L. G.; Mariscal, R.; Retuerto, M.; López Granados, M. Post-Synthesis Treatment of TS-1 with TPAOH: Effect of Hydrophobicity on the Liquid-Phase Oxidation of Furfural to Maleic Acid. *Top. Catal.* **2019**, *62* (5–6), 560–569.

(43) Hammond, C.; Conrad, S.; Hermans, I. Simple and Scalable Preparation of Highly Active Lewis Acidic Sn-β. *Angew. Chem., Int. Ed.* **2012**, *51* (47), 11736–11739.

(44) Brunauer, S.; Emmett, P. H.; Teller, E. Adsorption of Gases in Multimolecular Layers. *J. Am. Chem. Soc.* **1938**, *60* (2), 309–319.

(45) Datka, J.; Turek, A. M.; Jehng, J. M.; Wachs, I. E. Acidic Properties of Supported Niobium Oxide Catalysts: An Infrared Spectroscopy Investigation. *J. Catal.* **1992**, *135* (1), 186–199.

(46) Tang, B.; Dai, W.; Wu, G.; Guan, N.; Li, L.; Hunger, M. Improved Postsynthesis Strategy to Sn-Beta Zeolites as Lewis Acid Catalysts for the Ring-Opening Hydration of Epoxides. *ACS Catal.* **2014**, *4* (8), 2801–2810.

(47) Hammond, C.; Padovan, D.; Al-Nayili, A.; Wells, P. P.; Gibson, E. K.; Dimitratos, N. Identification of Active and Spectator Sn Sites in Sn-Beta Following Solid-State Stannation, and Consequences for Lewis Acid Catalysis. *ChemCatChem* **2015**, *7* (20), 3322–3331.

(48) Bhagwat, M.; Shah, P.; Ramaswamy, V. Synthesis of Nanocrystalline SnO_2 Powder by Amorphous Citrate Route. *Mater. Lett.* **2003**, *57* (9–10), 1604–1611.

(49) Gu, F.; Wang, S. F.; Song, C. F.; Lü, M. K.; Qi, Y. X.; Zhou, G. J.; Xu, D.; Yuan, D. R. Synthesis and Luminescence Properties of SnO_2 Nanoparticles. *Chem. Phys. Lett.* **2003**, *372* (3–4), 451–454.

(50) Pang, G.; Chen, S.; Koltypin, Y.; Zaban, A.; Feng, S.; Gedanken, A. Controlling the Particle Size of Calcined Sn02 Nanocrystals. *Nano Lett.* **2001**, *1* (12), 723–726.

(51) Moliner, M.; Roman-Leshkov, Y.; Davis, M. E. Tin-Containing Zeolites Are Highly Active Catalysts for the Isomerization of Glucose in Water. *Proc. Natl. Acad. Sci.* **2010**, *107* (14), 6164–6168.

(52) Corma, A.; Fornés, V.; Iborra, S.; Mifsud, M.; Renz, M. One-Pot Synthesis of Phenols from Aromatic Aldehydes by Baeyer-Villiger Oxidation with H_2O_2 Using Water-Tolerant Lewis Acids in Molecular Sieves. *J. Catal.* **2004**, *221* (1), 67–76.

(53) Renz, M.; Blasco, T.; Corma, A.; Fornés, V.; Jensen, R.; Nemeth, L. Selective and Shape-Selective Baeyer-Villiger Oxidations of Aromatic Aldehydes and Cyclic Ketones with Sn-Beta Zeolites and H_2O_2. *Chem. Eur. J.* **2002**, *8* (20), 4708–4717.

(54) Waidmann, C. R.; Dipasquale, A. G.; Mayer, J. M. Synthesis and Reactivity of Oxo-Peroxo-Vanadium(V) Bipyridine Compounds. *Inorg. Chem.* **2010**, *49* (5), 2383–2391.

(55) Shetti, V. N.; Manikandan, P.; Srinivas, D.; Ratnasamy, P. Reactive Oxygen Species in Epoxidation Reactions over Titanosilicate Molecular Sieves. *J. Catal.* **2003**, *216* (1), 461–467.

(56) Jianshuai Mu; Yan Wang; Min Zhao; Li Zhang. Intrinsic Peroxidase-like Activity and Catalase-like Activity of Co_3O_4 Nanoparticles. *Chem. Commun.* **2012**, *48* (19), 2540–2542.

(57) Chaiti Ray; Soumen Dutta; Sougata Sarkar; Ramkrishna Sahoo; Anindita Roy; Tarasankar Pal. Intrinsic Peroxidase-like Activity of Mesoporous Nickel Oxide for Selective Cysteine Sensing. *J. Mater. Chem. B* **2014**, *2* (36), 6097–6105.

(58) Huimin Jia; Dongfang Yang; Xiangna Han; Junhui Cai; Haiying Liu; Weiwei He. Peroxidase-like Activity of the Co_3O_4 Nanoparticles Used for Biodetection and Evaluation of Antioxidant Behavior. *Nanoscale* **2016**, *8* (11), 5938–5945.